university of groningen

University Medical Center Groningen

University of Groningen

Nanoscale temperature sensing using the Seebeck effect

Bakker, F. L.; Flipse, J.; van Wees, B. J.

Published in:
Journal of Applied Physics

DOI:
10.1063/1.3703675

IMPORTANT NOTE: You are advised to consult the publisher's version (publisher's PDF) if you wish to cite from it. Please check the document version below.

Document Version
Publisher's PDF, also known as Version of record

Publication date:
2012

Link to publication in University of Groningen/UMCG research database

Citation for published version (APA):
Bakker, F. L., Flipse, J., & van Wees, B. J. (2012). Nanoscale temperature sensing using the Seebeck effect. *Journal of Applied Physics*, *111*(8), 084306-1-084306-4. [084306]. https://doi.org/10.1063/1.3703675

Copyright
Other than for strictly personal use, it is not permitted to download or to forward/distribute the text or part of it without the consent of the author(s) and/or copyright holder(s), unless the work is under an open content license (like Creative Commons).

The publication may also be distributed here under the terms of Article 25fa of the Dutch Copyright Act, indicated by the "Taverne" license. More information can be found on the University of Groningen website: https://www.rug.nl/library/open-access/self-archiving-pure/taverne-amendment.

Take-down policy
If you believe that this document breaches copyright please contact us providing details, and we will remove access to the work immediately and investigate your claim.

Downloaded from the University of Groningen/UMCG research database (Pure): http://www.rug.nl/research/portal. For technical reasons the number of authors shown on this cover page is limited to 10 maximum.

Download date: 05-05-2023

Nanoscale temperature sensing using the Seebeck effect

F. L. Bakker,[a] J. Flipse, and B. J. van Wees
Physics of Nanodevices, Zernike Institute for Advanced Materials, University of Groningen, The Netherlands

(Received 13 January 2012; accepted 10 March 2012; published online 18 April 2012)

We experimentally study the effect of Joule heating on the electron temperature in metallic nanoscale devices and compare the results with a diffusive 3D finite element model. The temperature is probed using four thermocouples located at different distances from the heater. A good quantitative agreement, within 30%, between the experimental data and the modeling is obtained. Since we observe a strong thickness dependence of the electrical conductivity of our metals, we find that the Joule heating in nanoscale devices is often incorrectly calculated if bulk conductivities are used. Furthermore, Peltier heating/cooling is investigated and the combination with Seebeck temperature measurements provides us with a method to determine the Seebeck coefficient of a material. © *2012 American Institute of Physics*. [http://dx.doi.org/10.1063/1.3703675]

I. INTRODUCTION

Sensing and controlling heat flow in electronic devices becomes more important as the dimensions approach the nanoscale.[1] In contrast to charge transport, experimental studies of heat transport in mesoscopic structures are scarce,[2,3] though interesting new physics have been predicted. For example, electron-lattice relaxation processes can lead to a difference between phonon and electron temperatures at small length scales.[4] Moreover, the discovery of spin-dependent thermal effects,[5,6] e.g. the spin-Seebeck effect,[7] thermal spin injection,[8] and, very recently, the spin-dependent Peltier effect[9,10] has stimulated the interest in small scale heat flow control. Local temperature control and detection are crucial in the experimental study of these effects.

In this paper, we study local Joule heating in nanoscale strips by probing the electron temperature with thermocouples consisting of junctions between two different metals. We model the devices with 3D finite element methods in Comsol Multiphysics[11] and focus on the influence of the device dimensions on the transport behavior. Furthermore, the role of the substrate and the effect of electron-phonon scattering on the heat transport are discussed. By comparison of the measurement results with the model calculations, we aim for a better fundamental understanding of heat transport in nanoscale systems.

In quasi-equilibrium, when the device dimensions are much larger than the electron-electron relaxation length, the electron energy distribution is well defined. This distribution obeys Fermi-Dirac statistics and the system can be described in terms of a temperature T and a potential V. The conductivity is then energy-dependent, which leads to a gradient in the potential whenever a temperature gradient is present. This relation, $\nabla V = -S\nabla T$, is called the Seebeck effect and, for simple metals, S is given by the Mott relation,[12]

$$S = \frac{\pi^2}{3}\left(\frac{k_B^2 T}{e}\right)\left(\frac{\partial ln(\sigma(E))}{\partial E}\right)_{E=E_F}, \quad (1)$$

where σ is the electrical conductivity and E the electron energy. Since the Seebeck effect is a property of the electron system, it can be exploited for a temperature measurement of the electrons, for instance, by using a thermocouple (depicted in Fig. 1(a)). The Seebeck coefficient S is strongly material-dependent and has, for metals like Cu and Au, a rather small value ($\approx 2\ \mu V/K$). However, for Ni alloys, the effect is enhanced due to the specific band structure (up to $-40\ \mu V/K$ for NiCu).

II. EXPERIMENTAL TECHNIQUES

The samples are fabricated using a two-step electron beam lithography process on top of a thermally oxidized Si substrate with a SiO_2 layer thickness of 300 nm. A scanning electron microscopy (SEM) image of the device is shown in Fig. 1(b). The device consists of four 40-nm-thick $Ni_{45}Cu_{55}$ (Constantan) or Py ($Ni_{80}Fe_{20}$) strips that form a thermocouple with a 120-nm-thick top contact of Au. For the deposition of the NiCu, we use a double-layer resist technique with a large undercut area poly(methyl methacrylate-co-methacrylic acid) (PMMA-MA) (bottom layer: copolymer PMMA-MA, top-layer: PMMA 950 K) in combination with sputtering to preserve the right alloy composition. The Au and Py are deposited using an e-beam evaporator with a base pressure of 1×10^{-7} mbar. Prior to the deposition of Au, the NiCu or Py surface is cleaned with Ar ion milling to ensure transparent interfaces.

We have studied four types of devices, where we varied the heater material and its dimensions and the thermocouple materials. A heater consists of a metallic constriction that is electrically heated via Joule heating. It is connected by a metal strip to the four junction areas where we have measured the electron temperature. For the heating, an ac current with a low frequency (20 Hz) is used, which allows us to treat the heat transport as stationary for our device dimensions. The thermovoltages are measured using a lock-in measurement technique in order to separate linear ($\Delta T \propto I$) and quadratic ($\Delta T \propto I^2$) contributions, by taking the first harmonic V_1 and second harmonic V_2 response, respectively. In this way, we can separate the effects due to Joule heating (quadratic with the current) from other (linear) effects as, for

[a]Electronic mail: f.l.bakker@rug.nl.

 © 2012 American Institute of Physics

Downloaded 19 Apr 2012 to 129.125.63.113. Redistribution subject to AIP license or copyright; see http://jap.aip.org/about/rights_and_permissions

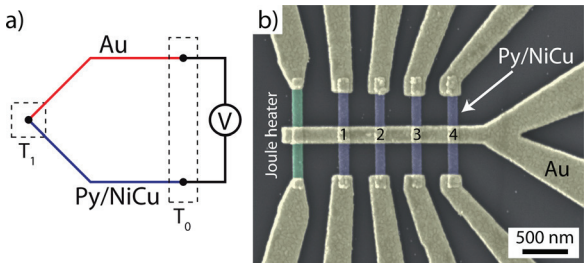

FIG. 1. (a) Schematic representation of a temperature measurement using a thermocouple. In our devices, we measure the difference between the electron temperature at junction of the two materials (T_1) and in the leads (T_0) by making use of the Seebeck effect. (b) Scanning electron microscope (SEM) image of the device. The temperature is locally increased using Joule heating in a narrow constriction (green). Consequently, a thermal gradient is generated across the Au strip and across the NiCu/Py strips. Via the Seebeck effect, this allows for an electron temperature measurement at each of the four interfaces (Refs. 1–4).

instance, the Peltier[13] or Nernst[11] effect. All measurements are performed at room temperature.

III. MODEL

The stationary heat transport is modeled based on Fourier's law, as described in earlier work.[11,13] In the model, both the charge current $\vec{J}$ and the heat current $\vec{Q}$ are coupled to the electrochemical potential eV and temperature T by the electrical conductivity σ, the thermal conductivity κ, Π, and S, via

$$\begin{pmatrix} \vec{J} \\ \vec{Q} \end{pmatrix} = -\begin{pmatrix} \sigma & \sigma S \\ \sigma\Pi & \kappa \end{pmatrix} \begin{pmatrix} \vec{\nabla} V \\ \vec{\nabla} T \end{pmatrix}. \quad (2)$$

The off-diagonal terms represent the Seebeck and Peltier effect, where $\Pi = ST_0$. Here, T_0 is the reference temperature of the device and taken to be 300 K. At the end of all the leads and at the bottom of the substrate, we set the temperature at T_0. Joule heating is incorporated using $\vec{\nabla} \cdot \vec{Q} = J^2/\sigma$ and charge conservation is put in by the constraint $\vec{\nabla} \cdot \vec{J} = 0$. As input for the model, we use for the metals the electrical conductivities that are experimentally determined in a dedicated device, whereas the thermal conductivities are derived from the Wiedemann-Franz law. The Seebeck coefficients of Au and Pt are taken from literature,[14] while the Seebeck coefficients of Py and NiCu are the only free parameters in the model. Heat conduction through the substrate is taken into account for a total substrate thickness of 300 nm.[15] All model input parameters are summarized in Table I.

In our nanoscale devices, both phonons and electrons participate in the heat transport. For metals, the thermal conductance κ can then be seen as the sum of the contribution of the electron (κ_e) and phonon (κ_p) system, if we assume that the electrons and phonons are at the same temperature, i.e., the electron-phonon coupling is strong. On the other hand, if the electron-phonon coupling is weak, the electron and phonon system temperature cannot equilibrate fast enough and, hence, at very short length scales, we can neglect the phonon contribution completely. In fact, since thermal transport in metals is dominated by electrons ($\kappa_e \gg \kappa_p$), and since we are heating and detecting only the electron system, we argue that a description based on solely the electron system ($\kappa = \kappa_e$) is sufficient in purely metallic systems.

TABLE I. Modeling parameters. Electrical conductivities σ are measured in a separate device, whereas the thermal conductivities κ are derived from σ and the literature values κ_l and σ_l using the Wiedemann-Franz law as $\kappa = \frac{\sigma}{\sigma_l}\kappa_l$. The Seebeck coefficients S of Au and Pt are taken from literature, whereas the coefficients of Py and NiCu are determined by comparing the experimental results with the model. The thermal conductivity for SiO_2 is obtained from phonon conduction.[15]

Mat.	t [nm]	σ [S/m]	κ [W/(mK)]	S [μV/K]
Au	40	1.8×10^7	120	1.7
Au	120	2.7×10^7	180	1.7
Pt	40	4.2×10^6	32	−5
Py	40	2.9×10^6	20	−18
NiCu	40	1.0×10^6	10	−30
SiO_2	300	1.0×10^{-13}	1.3	0

For the SiO_2 substrate, the situation is different, since the heat conduction in insulators is fully determined by the phonons ($\kappa = \kappa_p$). When heat transfer across metal-insulator interfaces is taken into account, electron-phonon coupling is essential, because heat needs to be transferred from the electrons (metal) to the phonons (insulator). For electron-phonon relaxation lengths comparable to the device dimensions, the modeling needs, in principle, to be extended with electron-phonon interactions.[16,17] However, since the electron-phonon interaction length is expected to be in the order of tens of nanometers in metals at room temperature, we have assumed that phonons and electrons have equal temperatures everywhere.

IV. RESULTS AND DISCUSSION

The main results of the electron temperature measurements are shown in Fig. 2, where we have used a Joule heating rms current of 1 mA. In the first row of the figure, the results for heater type 1 are shown. Heater type 1 consists of a 120-nm-thick Au strip as displayed in Fig. 2(d). The data obtained for heater type 2 are plotted in the second row of Fig. 2. This heater consists of a narrow strip with a thickness of 40 nm such that the heat is generated more locally (Fig. 2(g)). For both heaters, we have measured the second harmonic response voltage V_2, which, divided by I^2, gives us the second harmonic resistance R_2. These Seebeck voltages are measured at four contacts with respect to a reference voltage V_{ref} for two different thermocouples, namely Py/Au (triangles in Figs. 2(a) and 2(e)) and NiCu/Au (triangles in Figs. 2(b) and 2(f)). The corresponding temperature distributions obtained from the modeling are shown in Fig. 2(c) and Fig. 2(g), where we have observed that the maximum temperature for the thin heater is higher than for the thick heater. The dots in Figs. 2(a), 2(b), 2(e), 2(f) refer to the Seebeck voltages ($V - V_{ref}$) that are calculated with the model.

The experimental observations are in good quantitative agreement with the calculations. We have slightly adjusted ($< 25\%$ with respect to the literature values) the Seebeck coefficient of NiCu and Py to obtain a better agreement with the data (Table I). Since Joule heating scales inversely proportional with the conductivity of the material ($\vec{\nabla} \cdot \vec{Q} = J^2/\sigma$), a

Downloaded 19 Apr 2012 to 129.125.63.113. Redistribution subject to AIP license or copyright; see http://jap.aip.org/about/rights_and_permissions

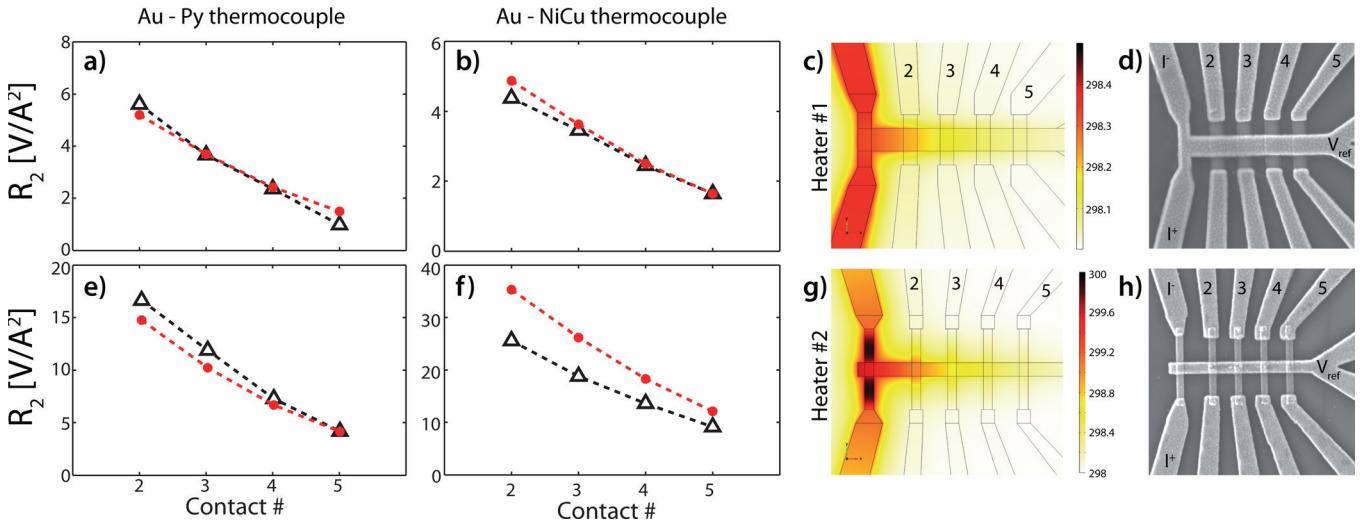

FIG. 2. (a) Seebeck voltage (triangles) at the different Py-Au thermocouples for a 120-nm-thick Au heater. (b) For a similar Joule heater as in a), but now with NiCu-Au thermocouples. (c) Modeling results for the device, where the obtained voltages are depicted in (a) and (b) (red dots). (d) SEM image of the device. (e) Py-Au thermocouple in combination with a 40-nm-thick Au heater strip. (f) NiCu-Au thermocouple with a heater consisting of 40-nm-thick Pt strip. (g) Temperature distribution obtained from thermoelectric modeling. (h) SEM image of the device.

correct value for the electrical conductivity is essential. Therefore, we have separately measured the conductivity for different materials and thicknesses. The results of these measurements are shown in Table I, where we have observed a thickness dependence for the electrical conductivity in Au. When this is taken into account, we find that our model is able to predict the Seebeck voltages fairly well. We note that the heat loss through the substrate plays a major role in these Joule-heated devices. Calculations without substrate lead to a mismatch up to one order of magnitude between experiment and theory. Furthermore, we have excluded magnetic effects by performing magnetic field-dependent measurements and did not find any dependence on magnetic field.

Figure 3 shows a similar measurement, where the heat source is changed from Joule heating to Peltier heating at one of the thermocouple interfaces. In the experiment, current is sent from contact I^+ to I^- and the first harmonic response voltage is measured at contacts 3, 4, and 5. Here, Joule heating is irrelevant, because that can only be observed in the second harmonic voltage response. The resistances ($R_1 = V_1/I$) are shown in Fig. 3(b) for a Py/Au thermocouple and in Fig. 3(c) for a NiCu/Au thermocouple. Again, we find a good agreement between the observations and the modeling, which confirms the validity of the diffusion model. Moreover, the observations are also in agreement with earlier measurements obtained in Py/Cu spin valves.[13]

The comparison between experiments and modeling of Joule heating presented in Fig. 2 emphasizes the importance of electrical conductivity measurements for all materials in the current path. For Peltier heating, which does not depend on the electrical conductivity, this requirement is not present and the modeling is often in better agreement with the data. For example, in Ref. 8 and Ref. 13, the observed Seebeck voltages generated by the Joule heating were up to three times higher than expected from modeling, whereas the Peltier heating could be modeled very well. We expect that the actual electrical conductivity of the materials in the current path was probably smaller and led to the mismatch between the model and experimental signals. The lower conductivities (compared to bulk) that are frequently observed in nanoscale devices and thin film multilayer structures are difficult to estimate and therefore require additional measurements.[18,19] Furthermore, the large surface to volume ratio of our nanosized contacts can lead to extra heat loss by thermal radiation to the environment, as reported by Léonard.[20] We did not observe this phenomenon, which can be explained by

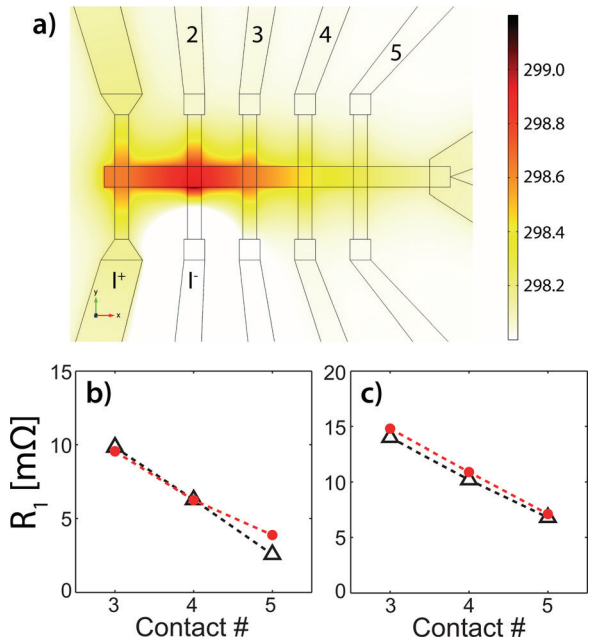

FIG. 3. Measurement of the Peltier heating and subsequent Seebeck voltage pick-up, where we exclude the effect of Joule heating by measuring solely the linear response voltage. (a) Modeling of the heating due to the Peltier effect for a current of 1 mA. In the temperature distribution shown, the effect of Joule heating is disregarded for clarity. (b) Results for the same device as discussed in Fig. 2(a). (c) Results for the same device as discussed in Fig. 2(b).

Downloaded 19 Apr 2012 to 129.125.63.113. Redistribution subject to AIP license or copyright; see http://jap.aip.org/about/rights_and_permissions

the fact that our device dimensions are still large compared to the nanowires considered in their article.

The thermoelectric model, in principle, allows for temperature-dependent parameters. However, in practice, little is known about their temperature dependence, which makes our model not directly applicable to temperatures other than room temperature. Moreover, the initial assumption that the electron-phonon interaction length is much smaller than the device dimensions is not necessarily valid at lower temperatures.[4] Small overall temperature variations, on the other hand, will not significantly alter the obtained results, since they can be assumed to be constant over the very short length scales measured here. Based on the minimum Seebeck voltage that is detectable (i.e., exceeds the noise level), we estimate that the highest sensitivity that can be obtained with these types of devices is a temperature difference of approximately 1 mK.

The agreement between our model and the experiment suggests that the initial assumption that electrons and phonons are at the same temperature everywhere is valid for the device dimensions discussed here. Additional experimental work is needed to study the heat transport across thin barriers of insulating material, as in, for example, tunnel barriers. In order to obtain accurate results, the modeling needs then to be extended with extra interface thermal conductances.[21]

V. CONCLUSION

In summary, we have presented an accurate measurement of the electron temperature in metallic nanoscale devices and compared it to finite-element modeling using Fourier's law based on diffusive transport. We found that the model was in good agreement with the experiments when the electrical conductivities of the materials are all well known. We allowed for small adjustments of the Seebeck coefficient from literature values for Py and NiCu to improve the agreement with the experiments. Furthermore, heat conduction through the substrate can be modeled accurately by assuming that the electron and phonon coupling is strong. We hope that this research stimulates further experimental investigation of nanoscale heat transport and, in particular, at smaller length- and timescales and by including nonmetallic elements.

ACKNOWLEDGMENTS

We would like to acknowledge B. Wolfs, M. de Roosz, and J. G. Holstein for technical assistance and I. J. Vera-Marun for critically reading the manuscript. This work is part of the research program of the Foundation for Fundamental Research on Matter (FOM) and supported by NanoLab, EU FP7 ICT Grant No. 257159 MACALO and the Zernike Institute for Advanced Materials.

[1]D. G. Cahill, W. K. Ford, K. E. Goodson, G. D. Mahan, A. Majumdar, H. J. Maris, R. Merlin, and S. R. Phillpot, "Nanoscale thermal transport," J. Appl. Phys. **93**, 793 (2003).
[2]A. D. Avery, R. Sultan, D. Bassett, D. Wei, and B. L. Zink, "Thermopower and resistivity in ferromagnetic thin films near room temperature," Phys. Rev. B **83**, 100401 (2011).
[3]W. Sun, H. Liu, W. Gong, L.-M. Peng, and S.-Y. Xu, "Unexpected size effect in the thermopower of thin-film stripes," J. Appl. Phys. **110**, 083709 (2011).
[4]F. Giazotto, T. Heikkilä, A. Luukanen, A. Savin, and J. Pekola, "Opportunities for mesoscopics in thermometry and refrigeration: Physics and applications," Rev. Mod. Phys. **78**, 217–274 (2006).
[5]G. E. Bauer, A. H. MacDonald, and S. Maekawa, "Spin Caloritronics," Solid State Commun. **150**, 459–460 (2010).
[6]M. Hatami, G. Bauer, Q. Zhang, and P. Kelly, "Thermoelectric effects in magnetic nanostructures," Phys. Rev. B **79**, 174426 (2009).
[7]K. Uchida, S. Takahashi, K. Harii, J. Ieda, W. Koshibae, K. Ando, S. Maekawa, and E. Saitoh, "Observation of the spin Seebeck effect." Nature **455**, 778–781 (2008).
[8]A. Slachter, F. L. Bakker, J.-P. Adam, and B. J. van Wees, "Thermally driven spin injection from a ferromagnet into a nonmagnetic metal," Nature Phys. **6**, 879–882 (2010).
[9]J. Flipse, F. L. Bakker, A. Slachter, F. K. Dejene, and B. J. van Wees, "Direct observation of the spin-dependent Peltier effect," Nat. Nanotechnol. **7**, 166–168 (2012).
[10]L. Gravier, S. Serrano-Guisan, F. Reuse, and J.-P. Ansermet, "Spin-dependent peltier effect of perpendicular currents in multilayered nanowires," Phys. Rev. B **73**, 052410 (2006).
[11]A. Slachter, F. L. Bakker, and B. J. van Wees, "Modeling of thermal spin transport and spin-orbit effects in ferromagnetic/nonmagnetic mesoscopic devices," Phys. Rev. B **84**, 174408 (2011).
[12]N. F. Mott and H. Jones, *The Theory of the Properties of Metals and Alloys* (Oxford University Press, London, 1936).
[13]F. L. Bakker, A. Slachter, J.-P. Adam, and B. J. van Wees, "Interplay of Peltier and Seebeck Effects in Nanoscale Nonlocal Spin Valves," Phys. Rev. Lett. **105**, 136601 (2010).
[14]C. Kittel, *Introduction to Solid State Physics*, 7th ed. (Wiley, New York, 1995).
[15]T. Yamane, N. Nagai, S. Katayama, and M. Todoki, "Measurement of thermal conductivity of silicon dioxide thin films using a 3ω method," J. Appl. Phys. **91**, 9772 (2002).
[16]J. Lai and A. Majumdar, "Concurrent thermal and electrical modeling of sub-micrometer silicon devices," J. Appl. Phys. **79**, 7353–7361 (1996).
[17]G. Chen, "Ballistic-diffusive heat-conduction equations," Phys. Rev. Lett. **86**, 2297–2300 (2001).
[18]K. Fuchs, "The conductivity of thin metallic films according to the electron theory of metals," Math. Proc. Cambridge Philos. Soc. **34**, 100–108 (1938).
[19]W. Steinhögl, G. Schindler, G. Steinlesberger, and M. Engelhardt, "Size-dependent resistivity of metallic wires in the mesoscopic range," Phys. Rev. B **66**, 075414 (2002).
[20]F. Léonard, "Reduced joule heating in nanowires," Appl. Phys. Lett. **98**, 103101 (2011).
[21]E. T. Swartz and R. O. Pohl, "Thermal resistance at interfaces," Appl. Phys. Lett. **51**, 2200–2202 (1987).

Downloaded 19 Apr 2012 to 129.125.63.113. Redistribution subject to AIP license or copyright; see http://jap.aip.org/about/rights_and_permissions